CONTENTS

JOURNAL OF RARE EARTHS
Vol. 36 No. 4 (April 2018)

CONTENTS

COMMUNICATIONS

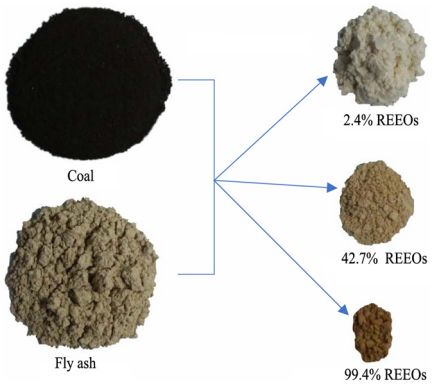

Various rare earth element oxides (REEOs) produced by Fan's group University of Wyoming (UW) from a fly ash (with 312 ppm REEs) generated with the combustion of a Powder River Basin (PRB) coal (containing 37 ppm REEs)

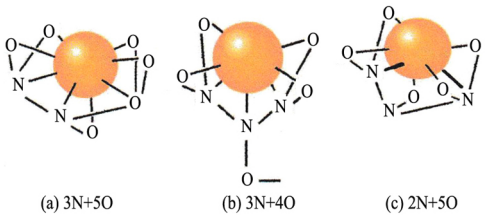

Possible structures of rare earth-DTPA complexes in aqueous solution

(a) La~Dy; (b) Ho~Yb,Y; (c) Lu

SPECTROSCOPY, LUMINESCENCE AND PHOSPHORS

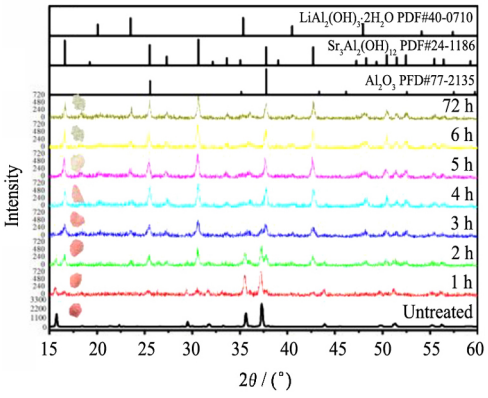

The charge of XRD patterns for $SrLiAl_3N_4:Eu^{2+}$ phosphor during the rapid degradation

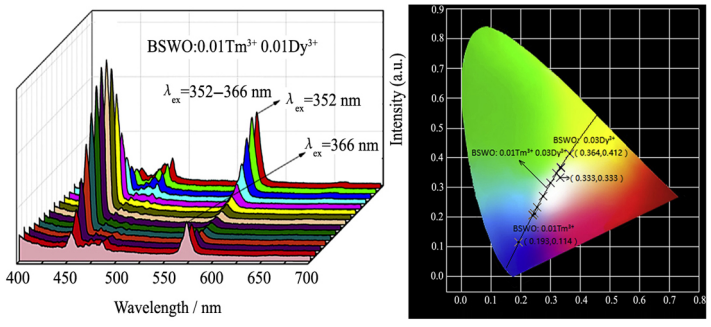

The emission spectra of BSWO:0.01Tm^{3+} 0.01Dy^{3+} and the CIE 1931 chromaticity diagram of BSWO:0.01Tm^{3+} 0.03Dy^{3+} excited at 352–366 nm

353 Oxalate-assisted morphological effect of $NaYF_4:Yb^{3+},Er^{3+}$ on photoelectrochemical performance for dye-sensitized solar cells

Juan Wang, Zhenqiang Du, Mirabbos Hojamberdiev, Siqi Zheng, Yunhua Xu

J. Rare Earths, (36) 2018: 353-358

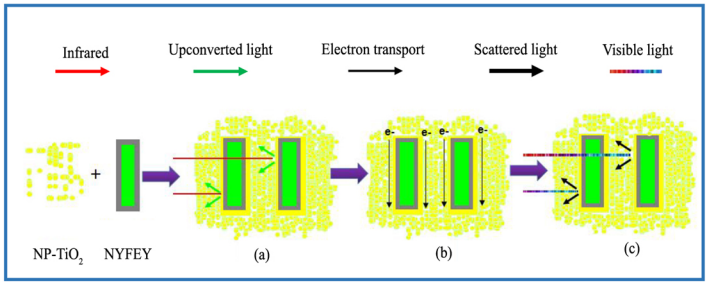

Function mechanisms of multifunctional composite photoanode prepared with NYFEY crystals with hexagonal rod-like structures

RARE EARTH CATALYSIS

359 Effect of hydration on the surface basicity and catalytic activity of Mg-rare earth mixed oxides for aldol condensation

Zheng Wang, Pascal Fongarland, Guanzhong Lu, Wangcheng Zhan, Nadine Essayem

J. Rare Earths, (36) 2018: 359-366

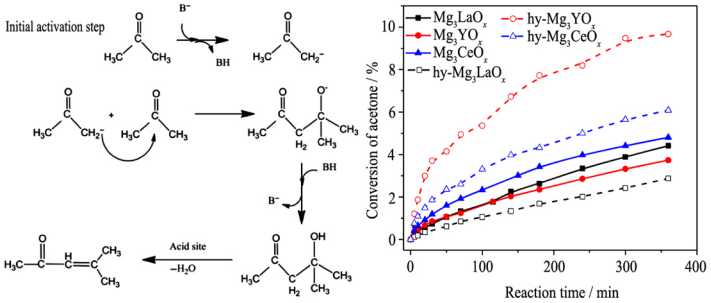

The Mg_3REO_x catalysts exhibit a high catalytic activity for aldol condensation of acetone, which is dependent on a homogeneous basic surface of medium strength. Upon hydration pre-treatment, the basic properties on the surface of the Mg_3REO_x catalysts were changed markedly, and the hy-Mg_3YO_x catalyst has the highest activity

367 Lanthanum incorporated in MCM-41 and its application as a support for a stable Ni-based methanation catalyst

Yang Han, Bo Wen, Mingyuan Zhu, Bin Dai

J. Rare Earths, (36) 2018: 367-373

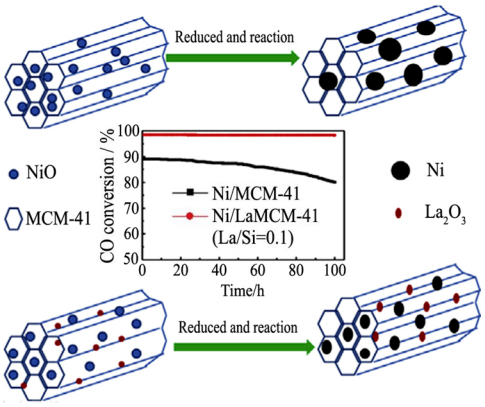

Lanthanum was incorporated via hydrothermal synthesis into a MCM-41 framework structure, the obtained Ni/LaMCM-41 catalyst exhibited excellent catalytic activity and stability for methanation. La reduces the average particle size of the NiO particles inhibits the sintering of the catalyst and the formation of carbon deposits

374 Preparation of Ce-TiO_2/carbon aerogel electrode and its performance in degradation of 4-chlorophenol

Yabo Wang, Zihong Pan, Dezhi Qin, Suzhen Bai, Qinlong Peng

J. Rare Earths, (36) 2018: 374-378

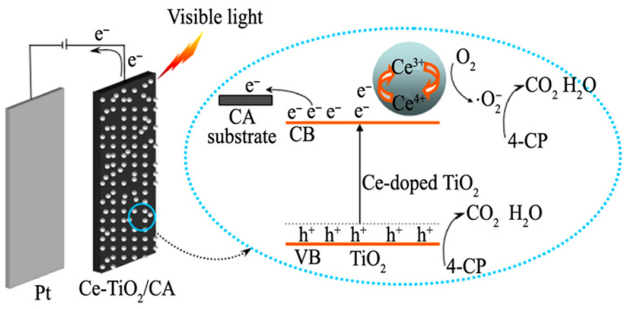

Ce-TiO_2/CA electrode is applied to treat a simulated 4-CP wastewater. The 4-CP molecules are efficiently degraded by the synergistic effect between electrosorption and photocatalysis

MAGNETISM AND MAGNETIC MATERIALS

379 Microstructure improvement related coercivity enhancement for sintered NdFeB magnets after optimized additional heat treatment

Qing Zhou, Wei Li, Yuan Hong, Lizhong Zhao, Xichun Zhong, Hongya Yu, Lili Huang, Zhongwu Liu

J. Rare Earths, (36) 2018: 379-384

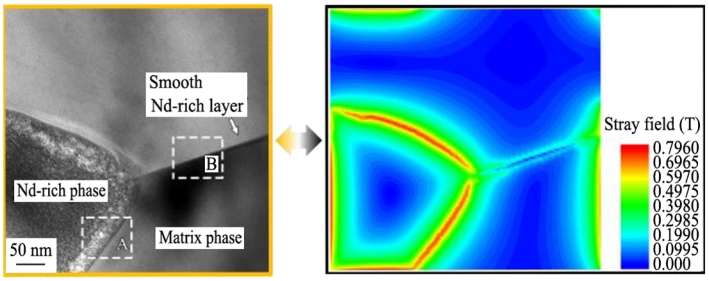

The distribution of the stray field corresponding to the beginning of the reversal process under the applied field approaches zero calculated from the surface in the model, which shows that the largest stray field exists at the intergranular phase. The presence of these non-ferromagnetic phases is expected to produce the magnetic stray field opposite to the spontaneous magnetization in the neighboring grains, thereby reduce the ideal nucleation field

385 Magnetic field stability of PrFeB magnets developed by GBD for cryogenic permanent magnet undulators

Yongzhou He, Xiaoqing Bao, Qiaogen Zhou

J. Rare Earths, (36) 2018: 385-389

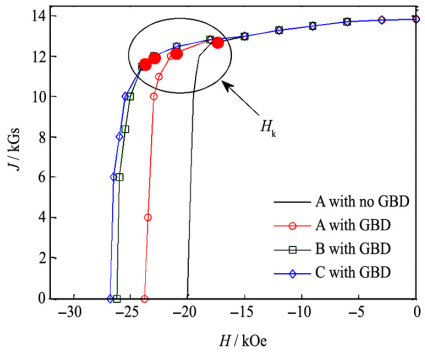

The magnetic properties of the PrFeB magnets with and without GBD. The B_r was approximately 13.85 kGs, and there were no obvious changes observed. However, the H_{cj} of the PrFeB magnets with GBD displayed a large increase in different degrees. The smaller orientation direction thickness of the magnet resulted in a larger increase of the H_{cj}. The comprehensive magnetic properties of the PrFeB magnets is about $(BH)_{max}+H_{cj}$=74.7

390 Effect of Nd^{3+} substitution on structural and magnetic properties of Mg–Cd ferrites synthesized by microwave sintering technique

S.R. Bhongale, H.R. Ingawale, T.J. Shinde, P.N. Vasambekar

J. Rare Earths, (36) 2018: 390-397

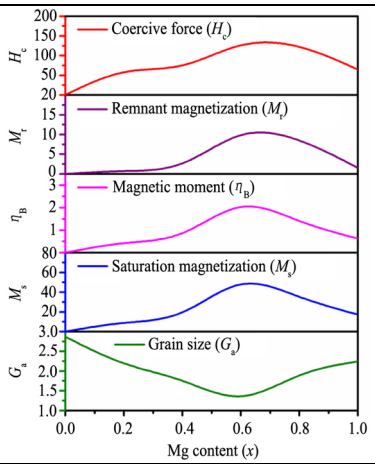

Variation of D, G_a, M_s, η_B, M_r, H_c with Mg-content for $Mg_xCd_{1-x}Nd_{0.03}Fe_{1.97}O_4$ (x=0.0, 0.2, 0.4, 0.6, 0.8 and 1.0) system

ADVANCED RARE EARTH MATERIALS

398 Helium ion irradiation effects on neodymium and cerium co-doped $Gd_2Zr_2O_7$ pyrochlore ceramic

Qijun Hu, Junsen Zeng, Lan Wang, Xiaoyan Shu, Dadong Shao, Haibin Zhang, Xirui Lu

J. Rare Earths, (36) 2018: 398-403

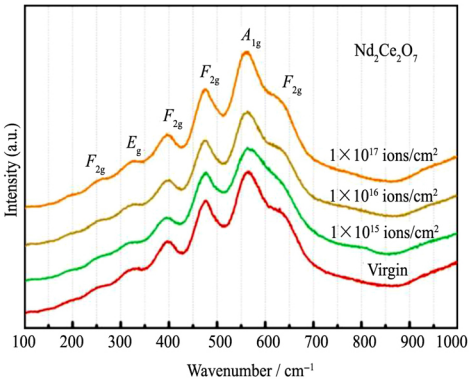

Raman spectra obtained from $Nd_2Ce_2O_7$ compositions before and after irradiation at various fluences from 1×10^{15} to 1×10^{17} ions/cm^2. The $Nd_2Ce_2O_7$ matrix keeps fluorite phase before and after irradiation at various fluences from 1×10^{15} to 1×10^{17} ions/cm^2, which present good irradiation tolerance

404 Sintering characteristics and microwave dielectric properties of $0.5Ca_{0.6}La_{0.267}TiO_3$-$0.5Ca(Mg_{1/3}Nb_{2/3})O_3$ ceramics prepared by reaction-sintering process

Jiamao Li, Peng Xu, Tai Qiu, Lichun Yao

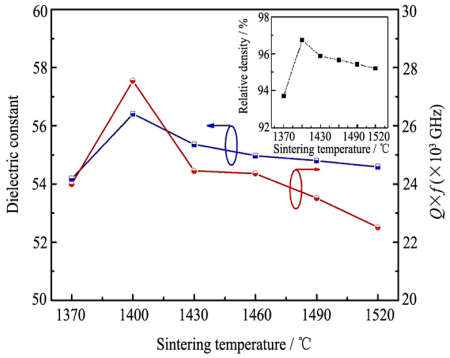

$0.5Ca_{0.6}La_{0.267}TiO_3$-$0.5Ca(Mg_{1/3}Nb_{2/3})O_3$ ceramics were successfully prepared by a reaction-sintering process. Fine microwave dielectric properties of ε_r=56.4, $Q\times f$=48550 GHz and τ_f=+8.7 ppm/°C for 5CLT-5CMN ceramics with high density sintered at 1400 °C for 4 h were obtained

J. Rare Earths, (36) 2018: 404-408

409 A comparison study of hydrogen storage performances of $SmMg_{11}Ni$ alloys prepared by melt spinning and ball milling

Yanghuan Zhang, Meng Ji, Zeming Yuan, Jingliang Gao, Yan Qi, Xiaoping Dong, Shihai Guo

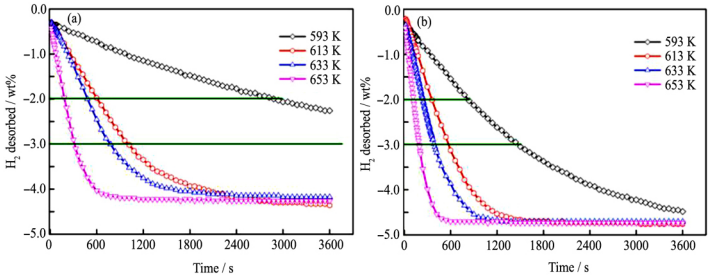

The as-milled alloy shows a much faster dehydriding rate. The time needed by desorbing 2 wt% H_2 at 593, 613, 633 and 653 K is 2940, 613, 484 and 185 s respectively for the as-spun alloy, while 848, 355, 232 and 132 s for the as-milled one

J. Rare Earths, (36) 2018: 409-417

CHEMISTRY AND HYDROMETALLURGY

418 Synthesis, characterization and cell imaging properties of rare earth compounds based on hydroxamate ligand

Linyan Yang, Yanping Zhang, Liwei Hu, Yunhe Zong, Ruili Zhao, Tianming Jin, Wen Gu

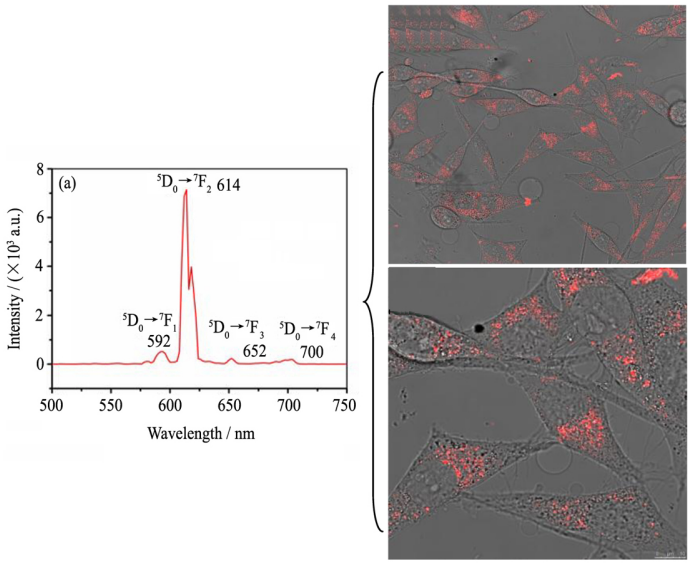

Six binuclear rare earth compounds have been synthesized through the ligand of sH_2bha. The fluorescence spectrum in the visible area showed characteristic peaks of Eu,Tb, and Dy compounds. The efficiency of Eu compound on the viability of PC3 cells was assessed using CCK8 assays

J. Rare Earths, (36) 2018: 418-423

METALLOGRAPHY AND PYROMETALLURGY

424 Microstructure and properties of as-cast Cu-Cr-Zr alloys with lanthanum addition

Jilin Li, Lili Chang, Shengli Li, Xinde Zhu, Zhongxin An

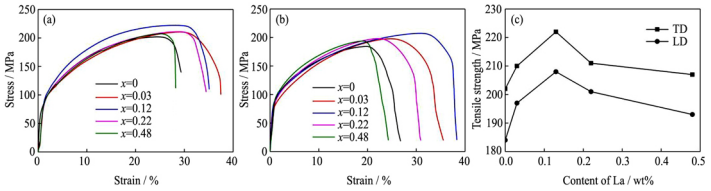

Room temperature stress strain curves along TD (a) and LD (b) and UTS (c) of Cu-0.45Cr-0.2Zr-*x*La alloys. Trace addition of La could refine grain size and clean grain boundaries, leading to the significant improvement of room temperature UTS, elongation while excessive addition of La severely harmed the performance of Cu-0.45Cr-0.2Zr-*x*La alloys. Besides, Cu-0.45Cr-0.2Zr-0.13La alloy possessed a good combination of room temperature UTS, elongation

J. Rare Earths, (36) 2018: 424-429

RARE EARTH APPLICATIONS

430 Exogenous rare earth element-yttrium deteriorated soil microbial community structure

Caigui Luo, Yangwu Deng, Jian Liang, Sipin Zhu, Zhenya Wei, Xiaobin Guo, Xianping Luo

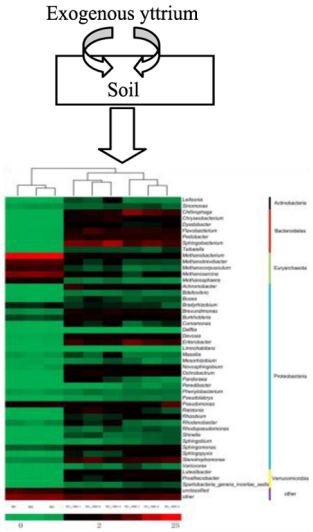

Exogenous yttrium deteriorated soil chemical properties and microbial community structure

J. Rare Earths, (36) 2018: 430-439

440 Effects of $CeCl_3$ and $LaCl_3$ on callus and root induction and the physical response of tobacco tissue culture

Guicheng Song, Pingping Zhang, Gaoling Shi, Huadun Wang, Hongxiang Ma

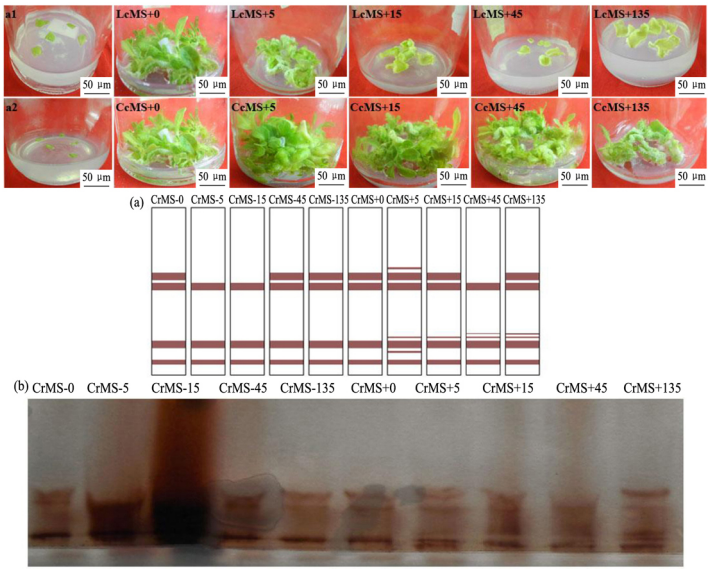

The enzyme activity and expression of related proteins are responsible for the increase in callus and root induction percentages at an optimal concentration of Ce^{3+} (<15 mg/L)

J. Rare Earths, (36) 2018: 440-448